Division for Meteorological and Atmospheric Research

- Precipitation measurements by advanced polarimetric radars and hydrometeor videosondes
- Development of new instrumental technology
- Clouds and precipitation observed by multiple satellites
- Millimeter-wave/infrared spectroscopy of green house gases and ozone-depleting substances
- Measurements and analyses of properties and behaviors of aerosols using advanced techniques

Ongoing global warming caused by increasing carbon dioxide concentrations and other greenhouse gases will cause gradual climate change and intensification of weather extremes and ecological catastrophes. Among the most urgent tasks for confronting global environmental problems more effectively is closely monitoring the atmosphere using different observation methods and gaining a better understanding of the atmosphere via theoretical insights and numerical modeling. To address these issues, the Division for Meteorological and Atmospheric Research is dedicated to several research projects to explore the atmosphere from various angles.

Main Activities in FY2020

New understanding of precipitation from MP-PAWR observations

Analytical research using a multi-parameter phased array weather radar (MP-PAWR) was conducted by taking advantage of MP-PAWR's "high-speed three-dimensional" observation, and studying the life cycle of isolated cumulonimbus clouds. The high temporal resolution observation data obtained from the MP-PAWR describe the life cycle of the cumulonimbus from the developing to the dissipating stage of the clouds; updraft was predominant in the entire cloud in the developing stage, and the maturity stage was characterized when the downdraft began to appear in the lower layer. During the mature stage, a core with high radar reflectivity was formed in the upper layer, which fell to the ground and produced heavy rain. Wet graupels were also present in the cores.

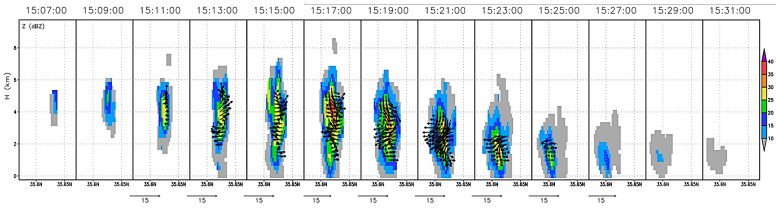

Life cycle of an isolated precipitation system with wind field.

Transient aggregation of convection: Observed behavior and underlying processes

Convective self-aggregation is among the most striking feature emerging from radiative-convective equilibrium simulations; however, its relevance to convective disturbances observed in the real atmosphere remains debatable. This study examined the observational signals of convective aggregation intrinsic to the life cycle of cloud clusters. The statistical evolution obtained from the satellite imagery showed that cloud clusters were gathered into fewer members during ±12 h as precipitation picked up. The high cloud cover per cluster expanded as the number of clusters

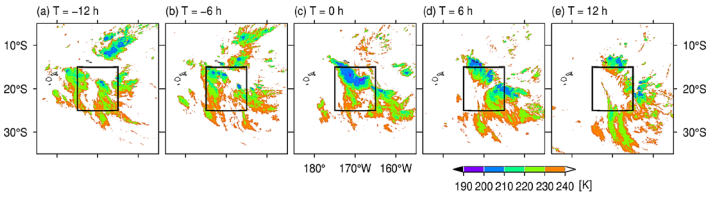

A series of snapshots of infrared brightness temperature illustrating an example of transient aggregation.

decreased, suggesting a transient occurrence of convective aggregation. An additional energy budget analysis was performed to explore the physical mechanisms of transient aggregation.

Impact of vertical profiles of water vapor in the upstream region of a heavy rainfall event in July 2018 in Japan

Vertical profiles of water vapor play a crucial role in rainfall amounts. A heavy rainfall event occurred in western Japan at the beginning of July 2018. The Japan Meteorological Agency (JMA) report showed that the convective activity in the upstream region over the East China Sea, approximately 1000 km away from the heavy rainfall region, should be moistening the middle troposphere, and a deep moist air-mass intrusion should have an important role in forming the event. This study explored the impact of vertical profiles of water vapor in the upstream region on the rainfall amount in western Japan using a Cloud Resolving Storm Simulator (CReSS) with a horizontal resolution of 2 km.

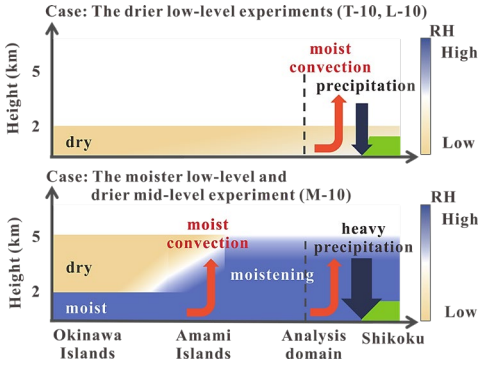

Schematic illustrations of impacts of vertical profiles of water vapor in the upstream region (around Okinawa Island) during the heavy rainfall event in western Japan.

The simulation captured the rainfall amount and its horizontal distribution well in western Japan. Trajectory analyses showed that the air mass intruding into western Japan had its origin in the upstream region around Okinawa Island. Sensitivity experiments that increase (decrease) the amount of water vapor in the lower troposphere in the upstream region showed the increasing (decreasing) rainfall amount in western Japan. However, no significant change in the rainfall amount in western Japan appeared in the sensitivity experiments that changed the amount of water vapor in the middle troposphere. In the drier experiment, convective activities along the trajectory moistened the middle troposphere, whereas in the moister experiments, convective activities along the trajectory removed water vapor in the middle troposphere by convective precipitation, and rainfall regions shifted to the upstream side. Therefore, precipitable water amounts in both the drier and moister experiments were approximately equal in western Japan. The results showed that the water vapor observation, especially in the lower troposphere, in the upstream region is important for forecasting the rainfall distribution and amount.

Observational study on the mesoscale structure inside an eye of a typhoon accompanying strong winds

Mesoscale structures, such as meso-vortices and polygonal eyes, have been observed inside the eye of typhoons in recent years and are an important topic for disaster prevention. When typhoon Trami (T1824) passed near Okinawa Island, the detailed structure inside its eye was observed using a polarimetric radar and phased-array radar. High wind was observed with a decreasing mixing ratio of water vapor in the vicinity of the eyewall clouds inside the eye, and the high wind region was in the polygonal eyewall clouds. Downward wind was estimated in the vicinity of the eyewall clouds inside the eye using Doppler analysis. The dry air above the inversion layer inside the eye should descend and transport a large momentum air-mass close to the eyewall clouds, and high wind with decreasing humidity should be observed inside the eye, and should be one of the formation mechanisms of high winds around the surface inside the eye.

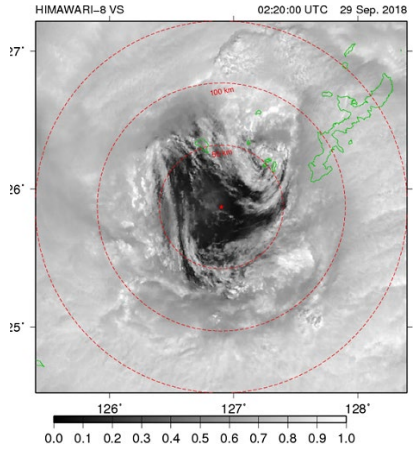

Visible image of the eye of the typhoon Trami obtained by the Geostationary Meteorological Satellite (Himawari-8) at 1120 JST on September 28, 2018. The shape of the eye is polygonal and a meso-vortex is located in the west of Okinawa Island.

Development of a new millimeter-wave superconducting device for multi-line observation in polar regions

We developed a new millimeter-wave superconducting mixing device for an observation project called "multi-line simultaneous observation of minor atmospheric molecules" in the polar regions via collaborative research with the Advanced Technology Center, NAOJ. The tuning circuit in the device was designed to match the characteristic impedance between the feed point and the superconducting tunnel junction in the frequency range of 180–250 GHz using an electromagnetic field and electrical circuit simulators. The devices were fabricated at the Advanced Technology Center, and their performances were measured in the laboratory at Nagoya University. The receiver noise temperature was lower than 50 K and 75 K from 200 to 240 GHz and 170 to 255 GHz, respectively. Therefore, we successfully developed a low-noise and wide-band device that was two times wider than previously in this frequency range.

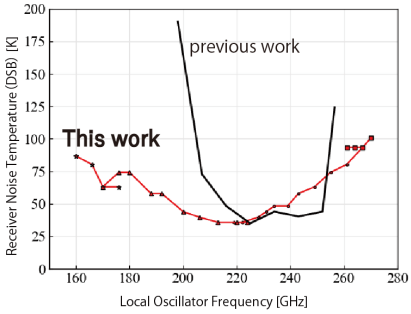

The noise temperature characteristics of the new millimeter-wave band superconducting receiver.

Observational studies on atmospheric composition changes caused by energetic particle precipitation in polar regions

To quantitatively understand the effects and mechanisms of the atmospheric composition changes caused by precipitating energetic charged particles into the middle atmosphere along the magnetic field due to solar activity, the ISEE installed millimeter-wave spectral radiometers at Syowa station in Antarctica and the EISCAT Tromsø site in Norway, and atmospheric minor constituents in the stratosphere and mesosphere were measured. At Syowa station, we have been conducting monitoring of nitric oxide (NO) and ozone (O_3) since January 2012 in collaboration with the NIPR. In 2020, a multi-frequency millimeter-wave spectral radiometer equipped with a waveguide multiplexer, a new IF circuit, and a 2-GHz band fast fourier transformation (FFT) spectrometer were established on-site, and simultaneous observations of O_3, NO, HO_2, and CO began in November 2020. This performance was confirmed adequate for monitoring. In February 2021, two microwave signal generators failed because of a sudden power failure, and after that, we observed O_3, NO, and HO_2. For the observations in Norway, in FY2020 we were unable to visit the site due to COVID-19 and could not conduct observations.

Understanding the relationships among chemical structure, sources, and atmospheric organic aerosol properties

For a precise understanding of the influences of atmospheric aerosols on air quality and climate, it is important to clarify the behaviors and properties of organic aerosol components, which have been poorly characterized to date. Studies focusing on the relationships among the chemical structure, sources, and atmospheric organic aerosol properties were performed. The relationship between the hygroscopic growth factor and the chemical structure of humic-like substances (HULIS) in aerosols collected in an urban area was analyzed, and the results suggest an association of the hygroscopicity parameter of HULIS

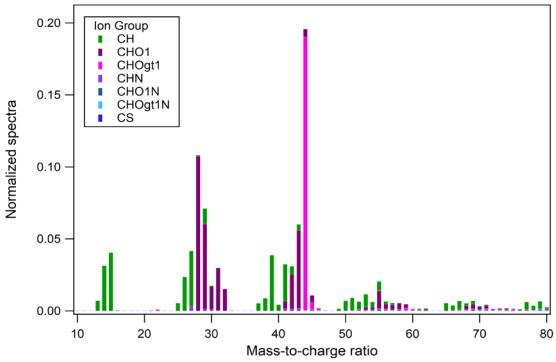

Aerosol mass spectrum obtained from the measurement of atomized atmospheric aerosol extract (HULIS) using an aerosol mass spectrometer. Information on chemical components can be obtained from the mass distribution measurement of ions generated by the collision of electrons with molecules in aerosol extract. The sample was collected at Tomakomai Experimental Forest, Hokkaido University. (The sample was provided by Dr. Miyazaki in Hokkaido University.)

with the chemical structure and source. The atmospheric concentrations of respective fractions in organic aerosol components were calculated based on the aerosol mass spectrometry of three fractions (e.g., HULIS) extracted from aerosol samples collected in a forest area. Precipitation and atmospheric aerosol samples were collected in an urban area, and the samples were subjected to excitation-emission matrix fluorescence spectroscopy and ultraviolet-visible spectroscopy, and the optical properties of the samples were analyzed. From chemical analysis of atmospheric aerosol samples collected in Australia, the atmospheric concentrations of chemical components were calculated, and basic data to analyze, for example, the properties of organic aerosols from forest fires were obtained. Ozonolysis experiments for ambient aerosols were performed to understand the aging of organic aerosols in the atmosphere, which is crucial for elucidating their atmospheric behaviors and properties.

Evaluation of methods to measure BC aerosols in the Arctic

In the Arctic, where the surface temperature increases more rapidly than the global average, forcing and feedback mechanisms associated with black carbon (BC) aerosols need to be elucidated. Most ground-based measurements of BC in the Arctic have been made using filter-based absorption photometers, such as particle soot absorption photometers (PSAP) and multi-angle absorption photometers (MAAP). These instruments measure the aerosol absorption coefficient (b_{abs}) and convert it to BC mass concentration (M_{BC}) by assuming the value of the mass absorption cross section (MAC). However, the accuracy of the conversion of babsbabs to M_{BC} has not been adequately assessed. In this study, we evaluated the MAC values at four Arctic sites by comparing b_{abs} measured by these instruments with M_{BC} independently measured by the continuous soot monitoring system (COSMOS). The accuracy of M_{BC} measured by the COSMOS has been previously demonstrated to be approximately 15% in the Arctic. We successfully estimated the MAC values for these instruments, which can be used to obtain error-constrained estimates of M_{BC} from babs measured at these sites, even in the past when COSMOS measurements were not made.

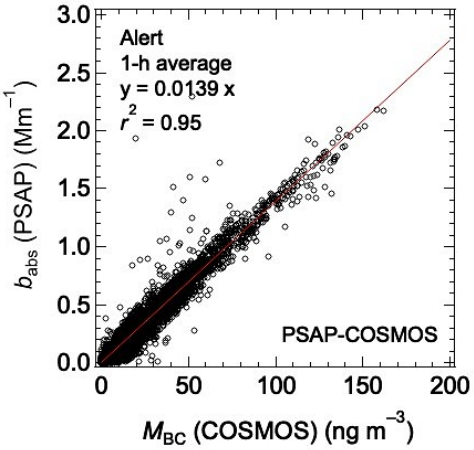

Correlation between M_{BC} (COSMOS) and b_{abs} (PSAP) at the observatory at Alert, Canada during 2018–2019. The slope of the least-squares fitted line represents the MAC value.